

Compact Triple Band-Notched UWB MIMO Antenna with Simple Stepped Stub to Enhance Wideband Isolation

Hui-Fen Huang* and Shu-Guang Xiao

Abstract—In this paper, a very compact ultra-wideband (UWB) multiple-input-multiple-output (MIMO) antenna, with a high isolation and triple notched bands, is proposed. Its size is dramatically decreased to $30 \times 26 \times 0.8 \text{ mm}^3$ on a cost-effective FR4 substrate. It consists of two rectangular printed monopole (PM) elements and a simple stepped ground stub to enhance wideband isolation. For two different rejected bands of the wireless local area network (WLANs) covering 5.15–5.35 and 5.725–5.825 GHz, four parasitic C-shaped split-ring resonators (PCSRRs) are placed on either side of the feed line. By etching two inverted U-shaped slots on the center of the patch, the notched frequency at 4 GHz C-band (3.7–4.2 GHz) of satellite communication systems is obtained. The results of simulation and measurement prove a bandwidth of $S_{11} < -10 \text{ dB}$ and $S_{12} < -21 \text{ dB}$ over the whole band (3.1–11.2 GHz) excluding the three independently adjustable rejection bands. Hence, the proposed UWB MIMO antenna has a very small size, simple structure, higher isolation and three narrower notched bands which effectively save more useful frequencies. Moreover, it is a good candidate for wireless portable UWB MIMO applications.

1. INTRODUCTION

Multiple-input-multiple-output (MIMO) technology [1, 2] can increase channel capacity substantially without adding frequency spectrum or input power. The ultra-wideband (UWB) [3] is a wireless communication technology possessing a large capacity and high-speed data rate for wireless portable device applications. Therefore, MIMO technology has been introduced to UWB antenna design for further increasing channel capacity [4]. In consideration of system interference, designing UWB MIMO antenna with several rejected bands is necessary, e.g., the wireless local area network (WLAN) covering 5.15–5.35 and 5.725–5.825 GHz, and 4 GHz C-band (3.7 to 4.2 GHz) of satellite communication systems [5].

Various planar UWB MIMO antennas with band-notched characteristics have been reported [6–9]. In [6], two rejected bands were achieved by parasitic strips and slots on the radiators. To reduce the mutual coupling at 3.0–4.0 GHz, a compact metal strip connected the two protruded ground parts. In [7], two rectangular radiators were utilized to satisfy the UWB. The decoupling structure, printed on the back side of the substrate, was connected to the patch by via in order to produce extra coupling path to reduce the original coupling energy between the two antenna elements. Moreover, two branches were added to this structure to form two notched bands. However, these two reported antennas were a little complicated and demanded relatively high fabrication accuracy. In [8] and [9], the rejected band at 5.15–5.85 GHz is achieved by etching two L-shaped slits and protruding two strips on the ground, respectively. However, the widths of the rejection bands are too wide, which leads to a waste of useful frequencies, especially the in-between band of lower and upper WLANs (5.35–5.725 GHz). Meanwhile, the effectiveness of the decoupling structures of these two reported antennas is not enough superior.

Received 14 August 2015, Accepted 10 September 2015, Scheduled 15 September 2015

* Corresponding author: Hui-Fen Huang (jia.luyang@mail.scut.edu.cn).

The authors are with the School of Electronic and Information Engineering, South China University of Technology, Guangzhou, China.

In this paper, a very compact UWB MIMO antenna, only occupying an area of $30 \times 26 \times 0.8 \text{ mm}^3$ including the ground plane, is proposed. It has a simple structure and can achieve three independently adjustable rejection bands. These three narrow rejected bands only cover the WLAN (5.15–5.35 GHz and 5.725–5.825 GHz), 4 GHz C-band (3.7–4.2 GHz) of satellite communication systems, but do not cover the in-between band of lower and upper WLANs (5.35–5.725 GHz) for saving useful frequencies. A simple stepped ground stub improves the isolation dramatically. Four parasitic C-shaped split-ring resonators (PCSRR), on either side of the feed line, are applied to reject two different bands of the WLAN (5.2- and 5.8-GHz). Two inverted U-shaped slots, etched on the center of the patch, are used to reject the band at 4 GHz C-band. The simulated and measured results show a bandwidth of $S_{11} < -10 \text{ dB}$ and $S_{12} < -21 \text{ dB}$ over the whole band (3.1–11.2 GHz) excluding three rejection bands and good diversity performances. Section 2 describes its design, and Section 3 analyses the working mechanism. In Section 4, the simulated and measured results of a prototype are discussed. Finally, the conclusion is presented in Section 5.

2. ANTENNA DESIGN

The UWB MIMO antenna, as shown in Figures 1 and 2, consists of two symmetric rectangular printed monopoles, denoted as PM1 and PM2, respectively. A simple stepped ground stub protrudes vertically between them to improve the isolation. Four PCSRRs on either side of feed line are used to reject WLAN (5.2- and 5.8-GHz). Two inverted U-shaped slots etched on the center of the patch, are used to reject 4 GHz C-band. It is not the shape but a large enough size of the radiator that produces a long current path in order to generate a low resonance for realizing the low-cutoff frequency of less than 3.1 GHz of the UWB. The basic resonant frequency of a proposed monopole antenna element could be approximated by [10]

$$f_r = \frac{144}{l_1 + l_2 + g + \frac{A_1}{2\pi l_1 \sqrt{\epsilon_{re}}} + \frac{A_2}{2\pi l_2 \sqrt{\epsilon_{re}}}}, \quad (1)$$

$$L = \frac{c}{2f_{\text{center}} \cdot \sqrt{\epsilon_{re}}}, \quad \text{where } \epsilon_{re} = \frac{\epsilon_r + 1}{2} \quad (2)$$

where A_1 and A_2 , l_1 and l_2 are the area and length of the ground and radiator, respectively; g is their gap, all in millimeters; ϵ_{re} is the effective dielectric constant. It is designed using High Frequency Structure Simulator [16] on FR4 substrate with dimensions of $30 \times 26 \text{ mm}^2$ and a relative permittivity of 4.4 and a loss tangent of 0.02 and a thickness of 0.8 mm. Parameters are (units in mm): $H = 0.8$ mm, $W = 30$, $W_{G2} = 3$, $W_{G3} = 4.2$, $W_{G4} = 8.8$, $W_r = 9.8$, $W_{r1} = 8$, $W_{r2} = 0.4$, $W_{C1} = 8$, $W_{C2} = 0.6$,

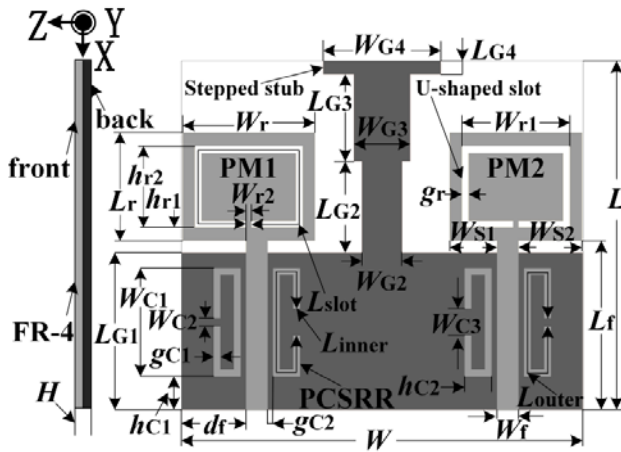


Figure 1. Geometry of the proposed antenna.

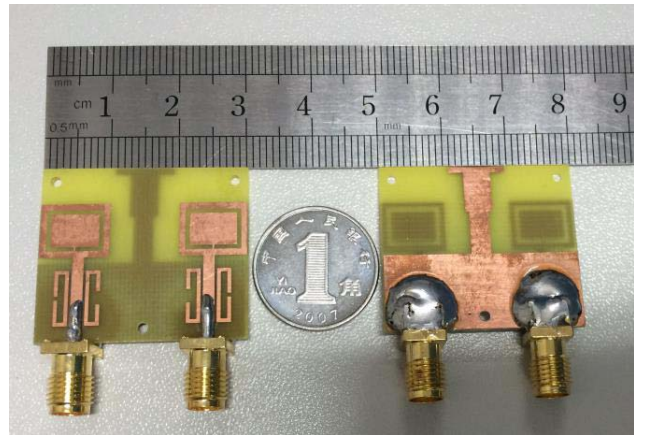


Figure 2. Fabrication prototype: top and bottom view.

$W_{C3} = 2$, $W_{S1} = 3.5$, $W_{S2} = 4.7$, $L = 26$, $L_{G1} = 11.7$, $L_{G2} = 6.8$, $L_{G3} = 6.5$, $L_{G4} = 1$, $L_f = 12.5$, $L_r = 8$, $h_{r1} = 1$, $h_{r2} = 6$, $h_{C1} = 2.5$, $h_{C2} = 2$, $g_r = 0.5$, $g_{C1} = 0.5$, $g_{C2} = 0.4$, $d_f = 4.9$.

3. MECHANISM ANALYSIS

3.1. Effects of the Simple Stepped Stub

In Figure 3, for better matching, a simple stepped stub protrudes vertically on the ground to decouple. It reflects radiation patterns of the two radiators and introduces more resonances generated by a monopole of this stub. So it leads a stronger current distribution to this stub, rather than be coupled to port 2 terminated with a 50 Ohm load. Moreover, by adjusting its size, the $S_{12} < -21$ dB and $S_{11} < -10$ dB in the whole band (3.1–11.2 GHz) are achieved. Also, using (1) in view of a single monopole, we have $l_1 = L$, $l_2 = L_r$, $g = L_f - L_{G1}$, $A_1 = L_{G1}W + L_{G2}W_{G2} + L_{G3}W_{G3} + L_{G4}W_{G4}$, and $A_2 = L_rW_r - (2W_{r1} - W_{r2} + 2h_{r2} - 4g_r)g_r$. The calculated result f_r is 3.88 GHz, close to the simulated result in Figure 4. (Sim — Simulation, Mea — Measurement, Ant-Antenna).

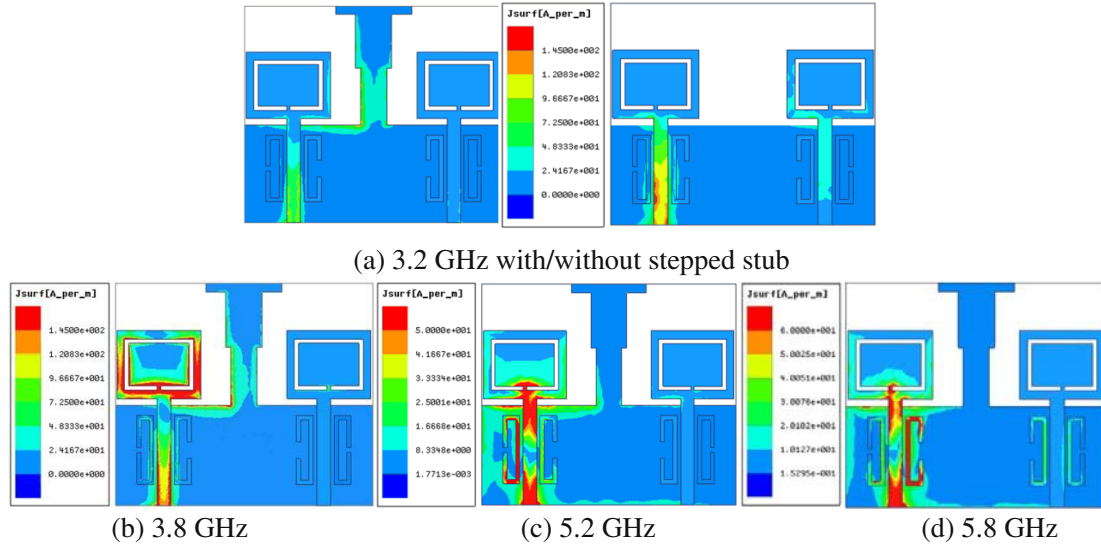


Figure 3. Current distribution: (a) 3.2 GHz w/o stepped stub, (b) 3.8 GHz, (c) 5.2 GHz, (d) 5.8 GHz.

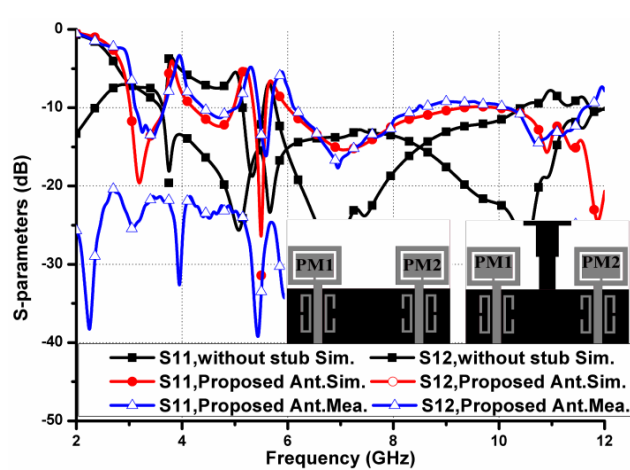


Figure 4. S -parameters with/without stepped stub.

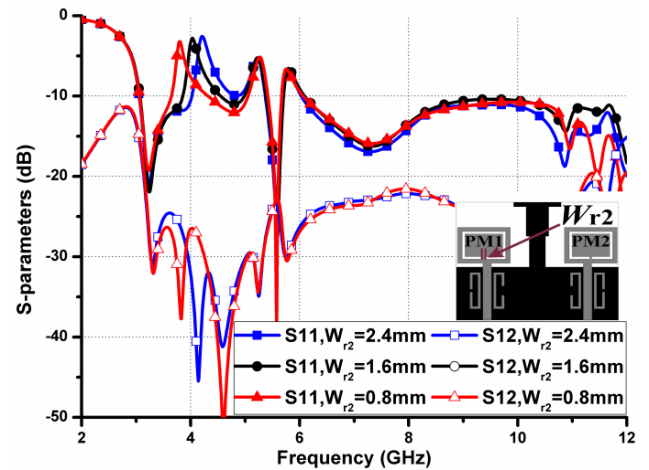


Figure 5. S -parameters with different values of W_{r2} .

3.2. Effects of PCSRRs and Etched Inverted U-Shaped Slots

UWB antennas can be considered as a series of some narrowband antennas which are equivalent to the series resonant RLC circuit [11] within a working frequency. Its equivalent impedance at the input terminal is

$$Z_e = \sum_{i=1}^n \frac{j\omega R_i L_i}{R_i(1 - \omega^2 L_i C_i) + j\omega L_i}, \quad (3)$$

The current distributions of Figures 3(b), (c), (d) indicate that the combination utilization of PCSRRs and etched slots generates three strong resonances at 3.8/5.2/5.8 GHz when port 1 is excited. Hence, three deep band notches are achieved. Using (2), the physical length of slots and PCSRRs ($L_{slot} = 2(W_{r1} + h_{r2} - 2g_r) - W_{r2} = 25.6 \text{ mm}/L_{outer} = 2(W_{C1} + h_{C2} - 2g_{C1}) - W_{C2} = 17.4 \text{ mm}/L_{inner} = 2(W_{C1} + h_{C2} - 2g_{C1}) - W_{C3} = 16 \text{ mm}$) are all approximately equal to $0.5\lambda_g$ at about 3.8/5.2/5.8 GHz (48/35.1/31.5 mm). Figures 5, 6 and 7 indicate that the longer the PCSRRs and slots are, the lower their corresponding resonant frequencies are. In other words, W_{r2} , W_{C2} and W_{C3} nearly independently control these three different rejection bands, although there still exists minimized coupling between PCSRRs and slots after we have optimized their shapes and positions.

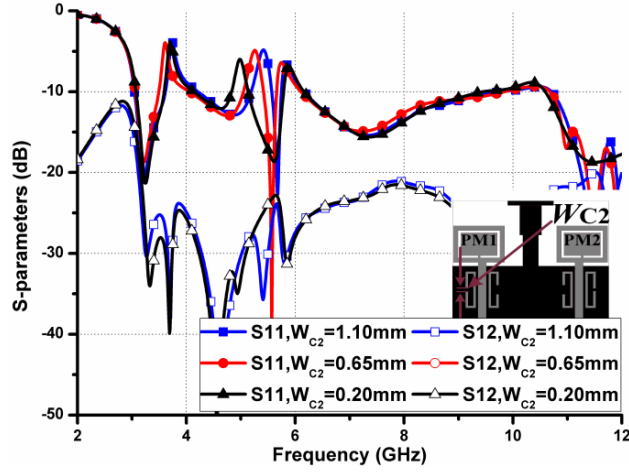


Figure 6. S -parameters with different values of W_{C2} .

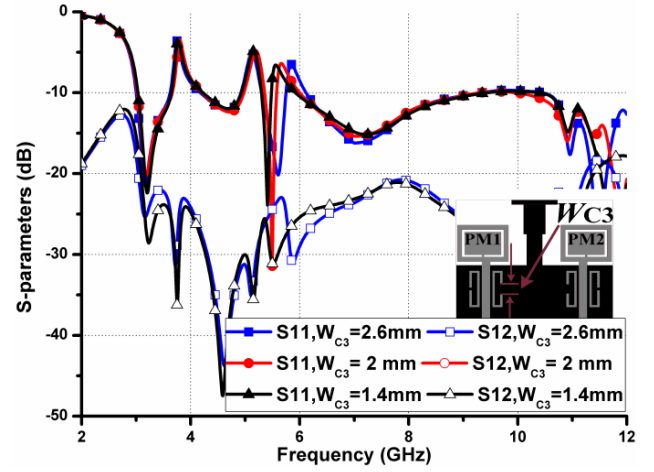


Figure 7. S -parameters with different values of W_{C3} .

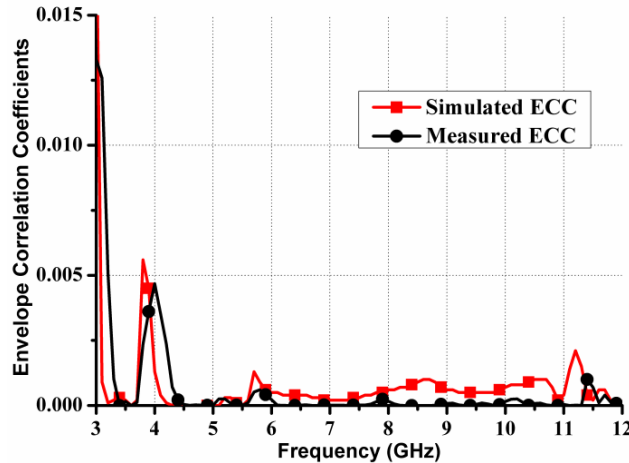


Figure 8. Simulated and measured ECC .

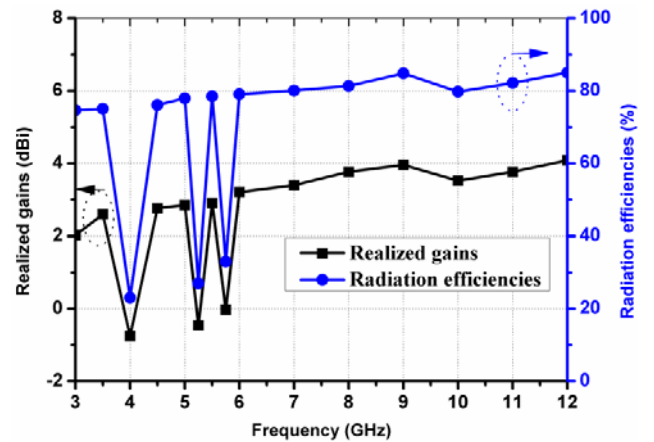


Figure 9. Measured realized gains and radiation efficiencies.

In Figure 4, the simulated and measured results show that a bandwidth of 3.1–11.2 GHz, with $S_{11} < -10$ dB, $S_{12} < -21$ dB, is achieved. Table 1 shows its superiority, e.g., the smaller size, higher isolation, wider band, more notched bands and different notch bands in the WLAN (5.2- and 5.8-GHz) for saving useful frequencies. Calculated from far-field radiation patterns [1], the envelope correlation coefficient (ECC) is below 0.02 in Figure 8, ensuring good diversity performances. In Figure 9, gains and efficiencies drop substantially in the notched bands, while gain ranges from 2 to 4 dBi and efficiency is above 70% in the rest of UWB. The field patterns at 3.2/5.5/8 GHz in Figure 10 shows good agreements. The patterns are nearly omni-directional in the Y - Z plane [7].

[illegible]

5. CONCLUSION

In this paper, a simple UWB MIMO antenna, with a small size of $30 \times 26 \times 0.8 \text{ mm}^3$ including the ground plane and triple independently adjustable notched bands, has been proposed, which can achieve a high isolation of $S_{12} < -21 \text{ dB}$ at 3.1–11.2 GHz with $S_{11} < -10 \text{ dB}$ and good diversity performances. Three rejected bands cover the WLAN (5.15–5.35 GHz and 5.725–5.825 GHz), 4 GHz C-band (3.7–4.2 GHz) of satellite communication systems, but do not cover the in-between band of lower and upper WLANs (5.35–5.725 GHz) typically. Hence, results show that our proposed antenna has a very small size, a simple structure, a higher isolation and three narrower notched bands which effectively save more useful frequencies. So it is promising for portable UWB MIMO applications.

ACKNOWLEDGMENT

This work is supported by the Department of Education of Guangdong Province Characteristic innovation Foundation 2014KTSCX017 and the National Natural Science Foundation of China under Grant 61071056.

REFERENCES

1. Vaughan, R. G. and J. B. Andersen, "Antenna diversity in mobile communication," *IEEE Trans. Veh. Technol.*, Vol. 36, No. 4, 149–172, Nov. 1987.
2. Zheng, L. and N. C. Tse, "Diversity and multiplexing: A fundamental tradeoff in multiple-antenna channels," *IEEE Trans. Inf. Theory*, Vol. 49, No. 5, 1073–1096, May 2003.
3. "Federal communications commission revision of part 15 of the commission's rules regarding ultra-wideband transmission system from 3.1 to 10.6 GHz," 98–153, Federal Communications Commission, Washington, D.C., ET-Docket, FCC, 2002.
4. Kaiser, T., F. Zheng, and E. Dimitrov, "An overview of ultra-wide-band systems with MIMO," *Proc. IEEE*, Vol. 97, No. 2, 285–312, Feb. 2009.
5. Jiang, D., Y. Xu, R. Xu, and W. Lin, "Compact dual-band-notched UWB planar monopole antenna with modified CSRR," *Electron. Lett.*, Vol. 48, No. 20, 1250–1252, Sep. 2012.
6. Li, J. F., Q. X. Chu, Z. H. Li, and X. X. Xia, "Compact dual band-notched UWB MIMO antenna with high isolation," *IEEE Trans. Antennas Propag.*, Vol. 61, No. 9, 4759–4766, Sep. 2013.
7. Tang, T. C. and K. H. Lin, "An ultrawideband MIMO antenna with dual band-notched function," *IEEE Antennas Wireless Propag. Lett.*, Vol. 13, 1076–1079, Jun. 2014.
8. Kang, L., H. Li, X. H. Wang, and X. W. Shi, "Compact offset microstrip-fed MIMO antenna for band-notched UWB application," *IEEE Antennas Wireless Propag. Lett.*, Vol. PP, No. 99, 1, 2015, DOI 10.1109/LAWP.2015.2422571.
9. Liu, L., S. W. Cheung, and T. I. Yuk, "Compact MIMO antenna for portable UWB applications with band-notched characteristic," *IEEE Trans. Antennas Propag.*, Vol. 63, No. 5, 1917–1924, May 2015.
10. Thomas, K. G. and M. Sreenivasan, "A simple ultrawideband planar rectangular printed antenna with band dispensation," *IEEE Trans. Antennas Propag.*, Vol. 58, No. 1, 27–34, Jan. 2010.
11. Lee, W.-S., D.-Z. Kim, K.-J. Kim, and J.-W. Yu, "Wideband planar monopole antennas with dual band-notched characteristics," *IEEE Trans. Microw. Theory Tech.*, Vol. 56, No. 12, 3637–3644, Dec. 2008.
12. Zhang, S., Z. Ying, J. Xiong, and S. He, "Ultrawideband MIMO/diversity antennas with a tree-like structure to enhance wideband isolation," *IEEE Antennas Wireless Propag. Lett.*, Vol. 8, 1279–1282, Dec. 2009.
13. Qin, H. and Y.-F. Liu, "Compact UWB MIMO antenna with ACS-fed structure," *Progress In Electromagnetics Research C*, Vol. 50, 29–37, 2014.

14. Khan, M. S., A. D. Capobianco, A. I. Najam, I. Shoaib, E. Autizi, and M. F. Shafique, "Compact ultra-wideband diversity antenna with a floating parasitic digitated decoupling structure," *IET Microw. Antenna and Propag.*, Vol. 8, No. 10, 747–753, Mar. 2014.
15. Khan, M. S., A. D. Capobianco, M. F. Shafique, B. Ijaz, A. Naqvi, and B. D. Braaten, "Isolation enhancement of a wideband MIMO antenna using floating parasitic elements," *Microw. Opt. Technol. Lett.*, Vol. 57, No. 7, 1677–1682, Jul. 2015.
16. Ansoft Corporation HFSS [Online], Available: <http://www.ansoft.com/products/hf/hfss/>.